

# EELBERT: Tiny Models through Dynamic Embeddings

Gabrielle Cohn, Rishika Agarwal, Deepanshu Gupta, and Siddharth Patwardhan

Apple

Cupertino, CA 95014

{gcohn,rishika\_agarwal,dkg,patwardhan.s}@apple.com

## Abstract

We introduce EELBERT, an approach for compression of transformer-based models (e.g., BERT), with minimal impact on the accuracy of downstream tasks. This is achieved by replacing the input embedding layer of the model with dynamic, i.e. on-the-fly, embedding computations. Since the input embedding layer accounts for a significant fraction of the model size, especially for the smaller BERT variants, replacing this layer with an embedding computation function helps us reduce the model size significantly. Empirical evaluation on the GLUE benchmark shows that our BERT variants (EELBERT) suffer minimal regression compared to the traditional BERT models. Through this approach, we are able to develop our smallest model UNO-EELBERT, which achieves a GLUE score within 4% of fully trained BERT-tiny, while being 15x smaller (1.2 MB) in size.

## 1 Introduction

It has been standard practice for the past several years for natural language understanding systems to be built upon powerful pre-trained language models, such as BERT (Devlin et al., 2019), T5 (Raffel et al., 2020), mT5 (Xue et al., 2021), and RoBERTa (Liu et al., 2019). These language models are comprised of a series of transformer-based layers, each transforming the representation at its input into a new representation at its output. Such transformers act as the “backbone” for solving several natural language tasks, like text classification, sequence labeling, and text generation, and are primarily used to map (or *encode*) natural language text into a multidimensional vector space representing the semantics of that language.

Experiments in prior work (Kaplan et al., 2020) have demonstrated that the size of the language model (i.e., the number of parameters) has a direct impact on task performance, and that increasing a language model’s size improves its language

understanding capabilities. Most of the recent state-of-art results in NLP tasks have been obtained with very large models. At the same time as massive language models are gaining popularity, however, there has been a parallel push to create much smaller models, which could be deployed in resource-constrained environments such as smart phones or watches.

Some key questions that arise when considering such environments: *How does one leverage the power of such large language models on these low-power devices? Is it possible to get the benefits of large language models without the massive disk, memory and compute requirements?* Much recent work in the areas of model pruning (Gordon et al., 2020), quantization (Zafir et al., 2019), distillation (Jiao et al., 2020; Sanh et al., 2020) and more targeted approaches like the *lottery ticket hypothesis* (Chen et al., 2020) aim to produce smaller yet effective models. Our work takes a different approach by reclaiming resources required for representing the model’s large vocabulary.

The inspiration for our work comes from Ravi and Kozareva (2018a), who introduced dynamic embeddings, i.e. embeddings computed on-the-fly via hash functions. We extend the usage of dynamic embeddings to transformer-based language models. We observe that 21% of the trainable parameters in BERT-base (Turc et al., 2019) are in the embedding lookup layer. By replacing this input embedding layer with embeddings computed at run-time, we can reduce model size by the same percentage.

In this paper, we introduce an “embeddingless” model – EELBERT – that uses a dynamic embedding computation strategy to achieve a smaller size. We conduct a set of experiments to empirically assess the quality of these “embeddingless” models along with the relative size reduction. A size reduction of up to 88% is observed in our experiments, with minimal regression in model quality, and this approach is entirely complementary to

other model compression techniques. Since EELBERT calculates embeddings at run-time, we do incur additional latency, which we measure in our experiments. We find that EELBERT’s latency increases relative to BERT’s as model size decreases, but could be mitigated through careful architectural and engineering optimizations. Considering the gains in model compression that EELBERT provides, this is not an unreasonable trade-off.

## 2 Related Work

There is a large body of work describing strategies for optimizing memory and performance of the BERT models (Ganesh et al., 2021). In this section, we highlight the studies most relevant to our work, which focus on reducing the size of the token embeddings used to map input tokens to a real valued vector representation. We also look at past research on hash embeddings or randomized embeddings used in language applications (e.g., Tito Svenstrup et al. (2017)).

Much prior work has been done to reduce the size of pre-trained static embeddings like GloVe and Word2Vec. Lebet and Collobert (2014) apply Principal Component Analysis (PCA) to reduce the dimensionality of word embedding. For compressing GloVe embeddings, Arora et al. (2018) proposed LASPE, which leverages matrix factorization to represent the original embeddings as a combination of basis embeddings and linear transformations. Lam (2018) proposed a method called Word2Bits that uses quantization to compress Word2Vec embeddings. Similarly, Kim et al. (2020) proposed using variable size code-blocks to represent each word, where the codes are learned via a feedforward network with binary constraint.

However, the most relevant works to this paper are by Ravi and Kozareva (2018b) and Ravi (2017). The key idea in the approach by Ravi and Kozareva (2018b) is the use of projection networks as a deterministic function to generate an embedding vector from a string of text, where this generator function replaces the embedding layer.

That idea has been extended to word-level embeddings by Sankar et al. (2021) and Ravi and Kozareva (2021), using an LSH-based technique for the projection function. These papers demonstrate the effectiveness of projection embeddings, combined with a stacked layer of CNN, BiLSTM and CRF, on a small text classification task. In our work, we investigate the potential of these pro-

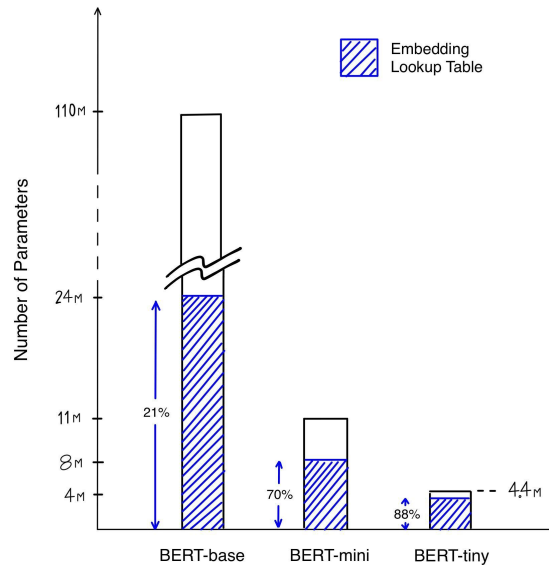


Figure 1: Embedding table in BERT

jection and hash embedding methods to achieve compression in transformer models like BERT.

## 3 Modeling EELBERT

EELBERT is designed with the goal of reducing the size (and thus the memory requirement) of the input embedding layers of BERT and other transformer-based models. In this section, we first describe our observations about BERT which inform our architecture choices in EELBERT, and then present the EELBERT model in detail.

### 3.1 Observations about BERT

BERT-like language models take a sequence of tokens as input, encoding them into a semantic vector space representation. The input tokens are generated by a tokenizer, which segments a natural language sentence into discrete sub-string units  $w_1, w_2, \dots, w_n$ . In BERT, each token in the model’s vocabulary is mapped to an index, corresponding to a row in the input embedding table (also referred to as the input embedding layer). This row represents the token’s  $d$ -size embedding vector  $\mathbf{e}_{w_i} \in \mathbb{R}^d$ , for a given token  $w_i$ .

The table-lookup-like process of mapping tokens in the vocabulary to numerical vector representations using the input embedding layer is a “non-trainable” operation, and is therefore unaffected by standard model compression techniques, which typically target the model’s trainable parameters. This results in a compression bottleneck, since a profiling of BERT-like models reveals that the input embedding layer occupies a large portion of the

model’s parameters.

We consider three publicly available BERT models of different sizes, all pre-trained for English (Turc et al., 2019) – *BERT-base*, *BERT-mini* and *BERT-tiny*. BERT-base has 12 layers with a hidden layer size of 768, resulting in about 110M trainable parameters. BERT-mini has 4 layers and a hidden layer size of 256, with around 11M parameters, and BERT-tiny has 2 layers and a hidden layer size of 128, totaling about 4.4M parameters.

Figure 1 shows the proportion of model size occupied by the input embedding layer (blue shaded portion of the bars) versus the encoder layers (unshaded portion of the bars). Note that in the smallest of these BERT variants, BERT-tiny, the input embedding layer occupies almost 90% of the model. By taking a different approach to model compression, focusing not on reducing the trainable parameters but instead on eliminating the input embedding layer, one could potentially deliver up to 9x model size reduction.

### 3.2 EELBERT Architecture

EELBERT differs from BERT only in the process of going from input token to input embedding. Rather than looking up each input token in the input embedding layer as our first step, we dynamically compute an embedding for a token  $w_i$  by using an  $n$ -gram pooling hash function. The output is a  $d$ -size vector representation,  $\mathbf{e}_{w_i} \in \mathbb{R}^d$ , just as we would get from the embedding layer in standard BERT. Keep in mind that EELBERT only impacts token embeddings, not the segment or position embeddings, and that all mentions of “embeddings” hereafter refer to token embeddings.

The key aspect of this method is that it does not rely on an input embedding table stored in memory, instead using the hash function to map input tokens to embedding vectors at runtime. This technique is not intended to produce embeddings that approximate BERT embeddings. Unlike BERT’s input embeddings, dynamic embeddings do not update during training.

Our  $n$ -gram pooling hash function methodology is shown in Figure 2, with operations in black boxes, and black lines going from the input to the output of those operations. Input and output values are boxed in blue. For ease of notation, we refer to the  $n$ -grams of length  $i$  as  $i$ -grams, where  $i = 1, \dots, N$ , and  $N$  is the maximum  $n$ -gram size. The steps of the algorithm are as follows:

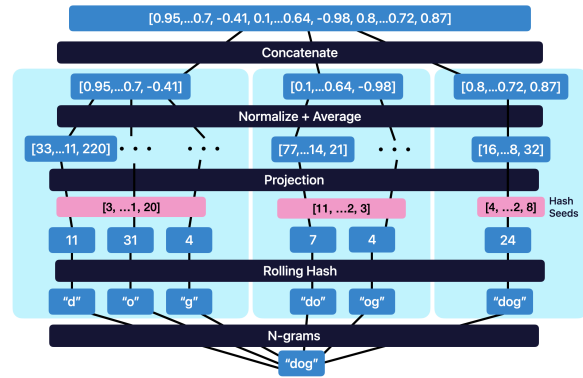


Figure 2: Computing dynamic hash embeddings

- 1. Initialize random hash seeds  $\mathbf{h} \in \mathbb{Z}^d$ .** There are  $d$  hash seeds in total, where  $d$  is the size of the embedding we wish to obtain, e.g. 768 for BERT-base. The  $d$  hash seeds are generated via a fixed random state, so we only need to save a single integer specifying the random state.
- 2. Hash  $i$ -grams to get  $i$ -gram signatures  $\mathbf{s}_i$ .** There are  $k_i = l - i + 1$  number of  $i$ -grams, where  $l$  is the length of the token. Using a rolling hash function (Wikipedia contributors, 2023), we compute the  $i$ -gram signature vectors,  $\mathbf{s}_i \in \mathbb{Z}^{k_i}$ .
- 3. Compute projection matrix for  $i$ -grams.** For each  $i$ , we compute a projection matrix  $\mathbf{P}_i$  using a subset of the hash seeds. The hash seed vector  $\mathbf{h}$  is partitioned into  $N$  vectors, boxed in pink in the diagram. Each partition  $\mathbf{h}_i$  is of length  $d_i$ , where  $\sum_{i=1}^N d_i = d$ , with larger values of  $i$  corresponding to a larger  $d_i$ . Given the hash seed vector  $\mathbf{h}_i$  and the  $i$ -gram signature vector  $\mathbf{s}_i$ , the projection matrix  $\mathbf{P}_i \in \mathbb{Z}^{k_i \times d_i}$  is the outer product  $\mathbf{s}_i \times \mathbf{h}_i$ . To ensure that the matrix values are bounded between  $[-1, 1]$ , we perform a sequence of transformations on  $\mathbf{P}_i$ :

$$\begin{aligned} \mathbf{P}_i &= \mathbf{P}_i \% B \\ \mathbf{P}_i &= \mathbf{P}_i - (\mathbf{P}_i > \frac{B}{2}) * B \\ \mathbf{P}_i &= \mathbf{P}_i / \frac{B}{2} \end{aligned}$$

where  $B$  is our bucket size (scalar).

- 4. Compute embedding,  $\mathbf{e}_i$ , for each  $i$ -grams.** We obtain  $\mathbf{e}_i \in \mathbb{R}^{d_i}$  by averaging  $\mathbf{P}_i$  across its  $k_i$  rows to produce a single  $d_i$ -dimensional vector.
- 5. Concatenate  $\mathbf{e}_i$  to get token embedding  $\mathbf{e}$ .**

We concatenate the  $N$  vectors  $\{\mathbf{e}_i\}_{i=1}^N$ , to get the token’s final embedding vector,  $\mathbf{e} \in \mathbb{R}^d$ .

For a fixed embedding size  $d$ , the tunable hyperparameters of this algorithm are:  $N$ ,  $B$ , and the

choice of the hashing function. We used  $N = 3$ ,  $B = 10^9 + 7$  and rolling hash function.

Since EELBERT replaces the input embedding layer with dynamic embeddings, the exported model size is reduced by the size of the input embedding layer:  $O(d \times V)$  where  $V$  is the vocabulary size, and  $d$  is the embedding size.

We specifically refer to the *exported size* here, because during pre-training, the model also uses an output embedding layer which maps embedding vectors back into tokens. In typical BERT pre-training, weights are shared between the input and output embedding layer, so the output embedding layer does not contribute to model size. For EELBERT, however, there is no input embedding layer to share weights with, so the output embedding layer does contribute to model size. Even if we pre-compute and store the dynamic token embeddings as an embedding lookup table, using the transposed dynamic embeddings as a frozen output layer would defeat the purpose of learning contextualized representations. In short, using coupled input and output embedding layers in EELBERT is infeasible, so BERT and EELBERT are the same size during pre-training. When pre-training is completed, the output embedding layer in both models is discarded, and the exported models are used for downstream tasks, which is when we see the size advantages of EELBERT.

## 4 Experimental Setup

In this section, we assess the effectiveness of EELBERT. The key questions that interest us are: *how much model compression can we achieve* and *what is the impact of such compression on model quality for language understanding?* We conduct experiments on a set of benchmark NLP tasks to empirically answer these questions.

In each of our experiments, we compare EELBERT to the corresponding standard BERT model – i.e., a model with the same configuration but with the standard trainable input embedding layer instead of our dynamic embeddings. This standard model serves as the baseline for comparison, to observe the impact of our approach.

### 4.1 Pre-training

For our experiments, we pre-train both BERT and EELBERT from scratch on the OpenWebText dataset (Radford et al., 2019; Gokaslan and Cohen, 2019), using the pre-training pipeline released

	BERT-base	EELBERT-base
Trainable Parameters	109,514,298	<b>86,073,402</b>
Exported Model Size	438 MB	<b>344 MB</b>
SST-2 (Acc.)	0.899	0.900
QNLI (Acc.)	0.866	0.864
RTE (Acc.)	0.625	0.563
WNLI* (Acc.)	0.521	0.563
MRPC (Acc., F1)	0.833, 0.882	0.838, 0.887
QQP* (Acc., F1)	0.898, 0.864	0.895, 0.861
MNLI (M, MM Acc.)	0.799, 0.802	0.790, 0.795
STSBB (P, S Corr.)	0.870, 0.867	0.851, 0.849
CoLA (M Corr.)	0.410	0.373
GLUE Score	0.775	0.760

Table 1: GLUE benchmark for BERT vs. EELBERT

by Hugging Face Transformers (Wolf et al., 2019). Each of our models is pre-trained for 900,000 steps with a maximum token length of 128 using the *bert-base-uncased* tokenizer. We follow the pre-training procedure described in Devlin et al. (2019), with a few differences. Specifically, (a) we use the OpenWeb Corpus for pre-training, while the original work used the combined dataset of Wikipedia and BookCorpus, and (b) we only use the *masked language model* pre-training objective, while the original work employed both *masked language model* and *next sentence prediction* objectives.

For BERT, the input and output embedding layers are coupled and trainable. Since EELBERT has no input embedding layer, its output embedding layer is decoupled and trainable.

### 4.2 Fine-tuning

For downstream fine-tuning and evaluation, we choose the GLUE benchmark (Wang et al., 2018) to assess the quality of our models. GLUE is a collection of nine language understanding tasks, including single sentence tasks (sentiment analysis, linguistic acceptability), similarity/paraphrase tasks, and natural language inference tasks. Using each of our models as a backbone, we fine-tune individually for each of the GLUE tasks under a setting similar to that described in Devlin et al. (2019). The metrics on these tasks serve as a proxy for the quality of the embedding models. Since GLUE metrics are known to have high variance, we run each experiment 5 times using 5 different seeds, and report the median of the metrics on all the runs, as done in Lan et al. (2020).

We calculate an overall GLUE score for each model. For BERT-base and EELBERT-base we use the following equation:

$$\text{AVERAGE}(\text{CoLA Matthews corr}, \text{SST-2 accuracy}, \text{MRPC accuracy}, \text{STSBB})$$



	<b>BERT-mini</b>	<b>EELBERT-mini</b>	<b>BERT-tiny</b>	<b>EELBERT-tiny</b>	<b>UNO-EELBERT</b>
Trainable Parameters	11,171,074	<b>3,357,442</b>	4,386,178	<b>479,362</b>	<b>312,506</b>
Exported Model Size	44.8 MB	<b>13.4 MB</b>	17.7 MB	<b>2.04 MB</b>	<b>1.24 MB</b>
SST-2 (Acc.)	0.851	0.835	0.821	0.749	0.701
QNLI (Acc.)	0.827	0.821	0.616	0.705	0.609
RTE (Acc.)	0.552	0.560	0.545	0.516	0.527
WNLI* (Acc.)	0.563	0.549	0.521	0.535	0.479
MRPC (Acc., F1)	0.701, 0.814	0.721, 0.814	0.684, 0.812	0.684, 0.812	0.684, 0.812
QQP* (Acc., F1)	0.864, 0.815	0.850, 0.803	0.780, 0.661	0.752, 0.712	0.728, 0.628
MNLI (M, M Acc.)	0.719, 0.730	0.688, 0.697	0.577, 0.581	0.582, 0.598	0.539, 0.552
CoLA (M Corr.)	0.103	0	0	0	0
GLUE score	0.753	0.746	0.671	0.666	0.632

Table 2: EELBERT with smaller models

Pearson corr, QQP accuracy, AVERAGE(MNLI match accuracy, MNLI mismatch accuracy), QNLI accuracy, RTE accuracy)

Like [Devlin et al. \(2019\)](#), we do not include the WNLI task in our calculations. For all the smaller BERT variants, i.e. BERT-mini, BERT-tiny, EELBERT-mini, EELBERT-tiny, and UNO-EELBERT, we use:

AVERAGE(SST-2 accuracy, MRPC accuracy, QQP accuracy, AVERAGE(MNLI match accuracy, MNLI mismatch accuracy), QNLI accuracy, RTE accuracy)

Note that we exclude CoLA and STSB from the smaller models’ score, because the models (both baseline and EELBERT) appear to be unstable on these tasks. We see a similar exclusion of these tasks in [Sun et al. \(2019\)](#).

Also note that in the tables we abbreviate MNLI match and mismatch accuracy as MNLI (M, MM Acc.), CoLA Matthews correlation as CoLA (M Corr.), and STSB Pearson and Spearman correlation as STSB (P, S Corr.).

## 5 Results

We present results of experiments assessing various aspects of the model with a view towards deployment and production use.

### 5.1 Model Size vs. Quality

Our first experiment directly assesses our dynamic embeddings by comparing the EELBERT models to their corresponding standard BERT baselines on GLUE benchmark tasks. We start by pre-training the models as described in Section 4.1 and fine-tune the models on downstream GLUE tasks, as described in Section 4.2.

Table 1 summarizes the results of this experiment. Note that replacing the trainable embedding

layer with dynamic embeddings does have a relatively small impact on the GLUE score. EELBERT-base achieves  $\sim 21\%$  reduction in parameter count while regressing by just 1.5% on the GLUE score.

As a followup to this, we investigate the impact of dynamic embeddings on significantly smaller sized models. Table 2 shows the results for BERT-mini and BERT-tiny, which have 11 million and 4.4 million trainable parameters, respectively. The corresponding EELBERT-mini and EELBERT-tiny models have 3.4 million and 0.5 million trainable parameters, respectively. EELBERT-mini has just 0.7% absolute regression compared to BERT-mini, while being  $\sim 3x$  smaller. Similarly, EELBERT-tiny is almost on-par with BERT-tiny, with 0.5% absolute regression, while being  $\sim 9x$  smaller.

Additionally, when we compare EELBERT-mini and BERT-tiny models, which have roughly the same number of trainable parameters, we notice that EELBERT-mini has a substantially higher GLUE score than BERT-tiny. This leads us to conclude that under space-limited conditions, it would be better to train a model with dynamic embeddings and a larger number of hidden layers rather than a shallower model with trainable embedding layer and fewer hidden layers.

### 5.2 Pushing the Limits: UNO-EELBERT

The results discussed in the previous section suggest that our dynamic embeddings have the most utility for extremely small models, where they perform comparably to standard BERT while providing drastic compression. Following this line of thought, we try to push the boundaries of model compression. We train UNO-EELBERT, a model with a similar configuration as EELBERT-tiny, but a reduced intermediate size of 128. We note that this model is almost 15 times smaller than BERT-tiny, with an absolute GLUE score regression of

Initialization Method	BERT-base		BERT-mini	
	<i>n</i> -gram pooling	random	<i>n</i> -gram pooling	random
Trainable Parameters	86,073,402	86,073,402	3,387,962	3,387,962
Exported Model Size	344 MB	344 MB	13.4 MB	13.4 MB
SST-2 (Acc.)	0.900	0.897	0.835	0.823
QNLI (Acc.)	0.864	0.862	0.821	0.639
RTE (Acc.)	0.563	0.574	0.560	0.569
WNLI* (Acc.)	0.563	0.507	0.549	0.507
MRPC (Acc., F1)	0.838, 0.887	0.806, 0.868	0.721, 0.814	0.690, 0.805
QQP* (Acc., F1)	0.895, 0.861	0.893, 0.858	0.850, 0.803	0.800, 0.759
MNLI (M, MM Acc.)	0.791, 0.795	0.786, 0.794	0.688, 0.697	0.647, 0.660
STS B (P, S Corr.)	0.851, 0.849	0.849, 0.847	-,-	-,-
CoLA (M Corr.)	0.373	0.389	0	0
GLUE score	0.760	0.757	0.746	0.696

Table 3: Impact of varying hash functions

Initialization Method	BERT-base	
	random	hash
Trainable Parameters	109,514,298	109,514,298
Exported Model Size	438 MB	438 MB
SST-2 (Acc.)	0.899	0.904
QNLI (Acc.)	0.866	0.876
RTE (Acc.)	0.625	0.614
WNLI* (Acc.)	0.521	0.563
MRPC (Acc., F1)	0.833, 0.882	0.850, 0.896
QQP* (Acc., F1)	0.898, 0.864	0.901, 0.867
MNLI (M, MM Acc.)	0.799, 0.802	0.807, 0.809
STS B (P, S Corr.)	0.870, 0.867	0.869, 0.867
CoLA (M Corr.)	0.410	0.417
GLUE score	0.775	0.780

Table 4: Initialization of trainable embeddings

less than 4%. It is also 350 times smaller than BERT-base, with an absolute regression of less than 20%. Note that for these regression calculations, all GLUE scores were calculated using the small-model GLUE score equation, which excludes CoLA and STSB, so that the scores would be comparable. We believe that with a model size of 1.2 MB, UNO-EELBERT could be a powerful candidate for low-memory edge devices like IoT, and other memory critical applications.

### 5.3 Impact of Hash Function

Our results thus far suggest that the trainable embedding layer can be replaced by a deterministic hash function with minimal impact on downstream quality. The hash function we used pools the *n*-gram features of a word to generate its embedding, so words with similar morphology, like "running" and "runner", will result in similar embeddings. In this experiment, we investigate whether our particular choice of hash function plays an important role in the model quality, or whether a completely random hash function which preserves no morphological information would yield similar results.

To simulate a random hash function, we initialize the embedding layer of BERT with a random normal distribution (BERT’s default initialization scheme), and then freeze the embedding layer, so each word in the vocabulary is mapped to a random embedding. The results presented in Table 3 indicate that for larger models like BERT-base, the hashing function doesn’t have much significance, as the models trained with random vs *n*-gram pooling hash functions perform similarly on the GLUE tasks. However, for the smaller BERT-mini model, our *n*-gram pooling hash function results in a better score. These results suggest that the importance of the *n*-gram pooling hash function, as compared to a completely random hash function, increases as the model size decreases. This is a useful finding, since the primary benefit of dynamic hashing is to develop small models that can be run on device.

### 5.4 Hash Function as Initializer

Based on the results of the previous experiment, we consider a potential alternative role for the embeddings generated by our hash function. We investigate whether our *n*-gram pooling hash function could be a better *initializer* for a trainable embedding layer, compared to the commonly used random normal distribution initializer. To answer this question, we conduct an experiment with BERT-base, by initializing one model with the default random normal initialization and the other model with the embeddings generated using our *n*-gram pooling hash function (*hash* column in Table 4). Note that in this experiment the input and output embedding layers are coupled, and embedding layers are trainable for both initialization schemes.

The results of this experiment are shown in Table 4. The hash-initialized model shows a 0.5% absolute increase in GLUE score compared to the

	BERT-base	EELBERT-base	BERT-mini	EELBERT-mini	BERT-tiny	EELBERT-tiny
Model Size (MB)	428.00	344.00	44.80	13.40	17.40	2.04
Latency (ms)	162.0	165.0	7.0	9.9	1.7	3.9

Table 5: Latency, on MacBookPro M1 32GB RAM

randomly-initialized model. We also perform this comparison for BERT-mini (not shown in the table), and observe a similar result. In fact, for BERT-mini, the hash-initialized model had an absolute increase of 1.6% in overall GLUE score, suggesting that the advantage of  $n$ -gram pooling hash-initialization may be even greater for smaller models.

### 5.5 Memory vs. Latency Trade-off

One consequence of using dynamic embeddings is that we are essentially trading off computation time for memory. The embedding lookup time for a token is  $O(1)$  in BERT models. In EELBERT, token embedding depends on the number of character  $n$ -grams in the token, as well as the size of the hash seed partitions. Due to the outer product between the  $n$ -gram signatures and the partitioned hash seeds, the overall time complexity is dominated by  $l \times d$ , where  $l$  is the length of a token, and  $d$  is the embedding size, leading to  $O(l \times d)$  time complexity to compute the dynamic hash embedding for a token. For English, the average number of letters in a word follows a somewhat Poisson distribution, with the mean being  $\sim 4.79$  (Norvig, 2012), and the embedding size  $d$  for BERT models typically ranging between 128 to 768.

The inference time for BERT-base vs EELBERT-base is practically unchanged, as the bulk of the computation time goes in the encoder blocks for big models with multiple encoder blocks. However, our experiments in Table 5 indicate that EELBERT-tiny has  $\sim 2.3x$  the inference time of BERT-tiny, as the computation time in the encoder blocks decreases for smaller models, and embedding computation starts constituting a sizeable portion of the overall latency. These latency measurements were done on a standard M1 MacBook Pro with 32GB RAM. We performed inference on a set of 10 sentences (with average word length of 4.8) for each of the models, reporting the average latency of obtaining the embeddings for a sentence (tokenization latency is same for all the models, and is excluded from the measurements).

To improve the inference latency, we suggest some architectural and engineering optimizations. The outer product between the  $O(l)$  dimensional  $n$ -

gram hash values and  $O(d)$  dimensional hash seeds, resulting in a matrix of size  $O(l \times d)$ , is the computational bottle-neck in the dynamic embedding computation. A sparse mask with a fixed number of 1’s in every row could reduce the complexity of this step to  $O(l \times s)$ , where  $s$  is the number of ones in each row, and  $s \ll d$ . This means every  $n$ -gram will only attend to some of the hash seeds. This mask can be learned during training, and saved with the model parameters without much memory overhead, as it would be of size  $O(k \times s)$ ,  $k$  being the max number of  $n$ -grams expected from a token. Future work could explore the effect of this approach on model quality. The hash embedding of tokens could also be computed in parallel, since they are independent of each other. Additionally, we observe that the 1, 2 and 3-grams follow a Zipf-ian distribution. By using a small cache of the embeddings for the most common  $n$ -grams, we could speed up the computation at the cost of a small increase in memory footprint.

## 6 Conclusions

In this work we explored the application of dynamic embeddings to the BERT model architecture, as an alternative to the standard, trainable input embedding layer. Our experiments show that replacing the input embedding layer with dynamically computed embeddings is an effective method of model compression, with minimal regression on downstream tasks. Dynamic embeddings appear to be particularly effective for the smaller BERT variants, where the input embedding layer comprises a larger percentage of trainable parameters.

We also find that for smaller BERT models, a deeper model with dynamic embeddings yields better results than a shallower model of comparable size with a trainable embedding layer. Since the dynamic embeddings technique used in EELBERT is complementary to existing model compression techniques, we can apply it in combination with other compression methods to produce extremely tiny models. Notably, our smallest model, UNO-EELBERT, is just 1.2 MB in size, but achieves a GLUE score within 4% of that of a standard fully trained model almost 15 times its size.

## References

- Sanjeev Arora, Yuanzhi Li, Yingyu Liang, Tengyu Ma, and Andrej Risteski. 2018. [Linear Algebraic Structure of Word Senses, with Applications to Polysemy](#). *Transactions of the Association for Computational Linguistics*, 6:483–495.
- Tianlong Chen, Jonathan Frankle, Shiyu Chang, Sijia Liu, Yang Zhang, Zhangyang Wang, and Michael Carbin. 2020. The Lottery Ticket Hypothesis for Pre-trained BERT Networks. *Advances in Neural Information Processing Systems*, 33:15834–15846.
- Jacob Devlin, Ming-Wei Chang, Kenton Lee, and Kristina Toutanova. 2019. [BERT: Pre-training of Deep Bidirectional Transformers for Language Understanding](#). In *Proceedings of the 2019 Conference of the North American Chapter of the Association for Computational Linguistics: Human Language Technologies, Volume 1 (Long and Short Papers)*, pages 4171–4186, Minneapolis, Minnesota. Association for Computational Linguistics.
- Prakhar Ganesh, Yao Chen, Xin Lou, Mohammad Ali Khan, Yin Yang, Hassan Sajjad, Preslav Nakov, Deming Chen, and Marianne Winslett. 2021. [Compressing Large-Scale Transformer-Based Models: A Case Study on BERT](#). *Transactions of the Association for Computational Linguistics*, 9:1061–1080.
- Aaron Gokaslan and Vanya Cohen. 2019. OpenWebText Corpus. <http://Skyllion007.github.io/OpenWebTextCorpus>.
- Mitchell Gordon, Kevin Duh, and Nicholas Andrews. 2020. Compressing BERT: Studying the Effects of Weight Pruning on Transfer Learning. In *Proceedings of the 5th Workshop on Representation Learning for NLP*, pages 143–155.
- Xiaoqi Jiao, Yichun Yin, Lifeng Shang, Xin Jiang, Xiao Chen, Linlin Li, Fang Wang, and Qun Liu. 2020. [TinyBERT: Distilling BERT for Natural Language Understanding](#). In *Findings of the Association for Computational Linguistics: EMNLP 2020*, pages 4163–4174, Online. Association for Computational Linguistics.
- Jared Kaplan, Sam McCandlish, Tom Henighan, Tom B. Brown, Benjamin Chess, Rewon Child, Scott Gray, Alec Radford, Jeffrey Wu, and Dario Amodei. 2020. [Scaling Laws for Neural Language Models](#). *arXiv*, abs/2001.08361.
- Yeachen Kim, Kang-Min Kim, and SangKeun Lee. 2020. [Adaptive Compression of Word Embeddings](#). In *Proceedings of the 58th Annual Meeting of the Association for Computational Linguistics*, pages 3950–3959, Online. Association for Computational Linguistics.
- Maximilian Lam. 2018. [Word2Bits - Quantized Word Vectors](#). *arXiv*, abs/1803.05651.
- Zhenzhong Lan, Mingda Chen, Sebastian Goodman, Kevin Gimpel, Piyush Sharma, and Radu Soricut. 2020. ALBERT: A Lite BERT for Self-supervised Learning of Language Representations. In *Proceedings of the Eighth International Conference on Learning Representations*.
- Rémi Lebreton and Ronan Collobert. 2014. [Word Embeddings through Hellinger PCA](#). In *Proceedings of the 14th Conference of the European Chapter of the Association for Computational Linguistics*, pages 482–490, Gothenburg, Sweden. Association for Computational Linguistics.
- Yinhan Liu, Myle Ott, Naman Goyal, Jingfei Du, Mandar Joshi, Danqi Chen, Omer Levy, Mike Lewis, Luke Zettlemoyer, and Veselin Stoyanov. 2019. [RoBERTa: A Robustly Optimized BERT Pretraining Approach](#). *arXiv*, abs/1907.11692.
- Peter Norvig. 2012. English Letter Frequency Counts: Mayzner Revisited or ETAOIN SRHLDCU. <http://norvig.com/mayzner.html>. [Online; accessed 23-October-2023].
- Alec Radford, Jeffrey Wu, Rewon Child, David Luan, Dario Amodei, Ilya Sutskever, et al. 2019. Language Models are Unsupervised Multitask Learners. *OpenAI Blog*, 1(8):9.
- Colin Raffel, Noam Shazeer, Adam Roberts, Katherine Lee, Sharan Narang, Michael Matena, Yanqi Zhou, Wei Li, and Peter J Liu. 2020. Exploring the Limits of Transfer Learning with a Unified Text-to-Text Transformer. *The Journal of Machine Learning Research*, 21(1):5485–5551.
- Sujith Ravi. 2017. [ProjectionNet: Learning Efficient On-Device Deep Networks Using Neural Projections](#). *arXiv*, abs/1708.00630.
- Sujith Ravi and Zornitsa Kozareva. 2018a. Self-governing neural networks for on-device short text classification. In *Proceedings of the 2018 Conference on Empirical Methods in Natural Language Processing*, pages 887–893.
- Sujith Ravi and Zornitsa Kozareva. 2018b. [Self-Governing Neural Networks for On-Device Short Text Classification](#). In *Proceedings of the 2018 Conference on Empirical Methods in Natural Language Processing*, pages 804–810, Brussels, Belgium. Association for Computational Linguistics.
- Sujith Ravi and Zornitsa Kozareva. 2021. [SoDA: On-device Conversational Slot Extraction](#). In *Proceedings of the 22nd Annual Meeting of the Special Interest Group on Discourse and Dialogue*, pages 56–65, Singapore and Online. Association for Computational Linguistics.
- Victor Sanh, Lysandre Debut, Julien Chaumond, and Thomas Wolf. 2020. [DistilBERT, a distilled version of BERT: smaller, faster, cheaper and lighter](#). *arXiv*, abs/1910.01108.



- Chinnadhurai Sankar, Sujith Ravi, and Zornitsa Kozareva. 2021. ProFormer: Towards On-Device LSH Projection Based Transformers. In *Proceedings of the 16th Conference of the European Chapter of the Association for Computational Linguistics: Main Volume*, pages 2823–2828.
- Siqi Sun, Yu Cheng, Zhe Gan, and Jingjing Liu. 2019. Patient Knowledge Distillation for BERT Model Compression. *arXiv*, abs/1908.09355.
- Dan Tito Svenstrup, Jonas Hansen, and Ole Winther. 2017. Hash Embeddings for Efficient Word Representations. *Advances in Neural Information Processing Systems*, 30:4935–4943.
- Iulia Turc, Ming-Wei Chang, Kenton Lee, and Kristina Toutanova. 2019. Well-Read Students Learn Better: On the Importance of Pre-training Compact Models. *arXiv*, abs/1908.08962.
- Alex Wang, Amanpreet Singh, Julian Michael, Felix Hill, Omer Levy, and Samuel Bowman. 2018. GLUE: A Multi-Task Benchmark and Analysis Platform for Natural Language Understanding. In *Proceedings of the 2018 EMNLP Workshop BlackboxNLP: Analyzing and Interpreting Neural Networks for NLP*, pages 353–355.
- Wikipedia contributors. 2023. Rolling hash — Wikipedia, The Free Encyclopedia. [https://en.wikipedia.org/w/index.php?title=Rolling\\_hash&oldid=1168768744](https://en.wikipedia.org/w/index.php?title=Rolling_hash&oldid=1168768744). [Online; accessed 23-October-2023].
- Thomas Wolf, Lysandre Debut, Victor Sanh, Julien Chaumond, Clement Delangue, Anthony Moi, Pierric Cistac, Tim Rault, Rémi Louf, Morgan Funtowicz, et al. 2019. Huggingface’s Transformers: State-of-the-Art Natural Language Processing. *arXiv preprint arXiv:1910.03771*.
- Linting Xue, Noah Constant, Adam Roberts, Mihir Kale, Rami Al-Rfou, Aditya Siddhant, Aditya Barua, and Colin Raffel. 2021. mT5: A Massively Multilingual Pre-trained Text-to-Text Transformer. In *Proceedings of the 2021 Conference of the North American Chapter of the Association for Computational Linguistics: Human Language Technologies*, pages 483–498.
- Ofir Zafrir, Guy Boudoukh, Peter Izsak, and Moshe Wasserblat. 2019. Q8BERT: Quantized 8Bit BERT. In *2019 Fifth Workshop on Energy Efficient Machine Learning and Cognitive Computing - NeurIPS Edition (EMC2-NIPS)*, pages 36–39, Vancouver, Canada. IEEE.